Displacement analysis of the interior walls of a pipe using panoramic holo-interferometry

by

John A. Gilbert
Department of Mechanical Engineering
University of Alabama in Huntsville
Huntsville, Alabama 35899

Donald R. Matthys
Physics Department
Marquette University
Milwaukee, Wisconsin 53233

Christelle M. Hendren
Department of Mechanical Engineering
University of Alabama in Huntsville
Huntsville, Alabama 35899

ABSTRACT

Standard phase-displacement equations, used for both double exposure and real time holo-interferometry, are combined with the geometrical mapping and optical characteristics of panoramic annular lenses to accurately measure surface displacement on the interior wall of a pipe. In this approach, one panoramic annular lens is used to illuminate the surface with coherent light, and the resulting intensity distribution is holographically recorded through a second panoramic annular lens. Interference fringes are obtained in real-time by comparing holograms recorded before and after the pipe is displaced. The annular images and the holographic fringes are acquired and stored digitally in a computer system. Image transformation algorithms are applied to remove optical distortions in the holographic pattern and fringe loci are compared to those predicted on the basis of theory.

1. INTRODUCTION

Holography is a technique for recording the three-dimensional information of an object on a two-dimensional photosensitive recording medium such that when the hologram is reconstructed or "played back" the original object can be viewed in its original three-dimensional form. The process requires two beams of light with a stable synchronized relationship which are conveniently obtained by splitting the light from a single laser into two parts. One light beam is used to illuminate the test surface and the corresponding object wavefront is diffused to the recording medium. The other light beam is expanded to form a reference wavefront which illuminates the recording medium directly. Mutual interference between these two highly coherent wavefronts is recorded as a complex diffraction grating. Once developed, the photosensitive medium is called a hologram and can be reconstructed by illuminating it with the reference beam. During reconstruction, the original object and associated optics can be completely removed. The reference beam is diffracted by the hologram to form a virtual image of the object.

Unlike ordinary photography where only the amplitude of the light intensity is recorded, the holographic process records both the phase and amplitude of the light scattered from an object. Phase information is important, since comparisons can be made between holograms recorded as a test surface moves. This process, called holo-interferometry,[1-4] produces a set of interference fringes which may permit the detection and measurement of surface displacement.

Significant progress has been made in the development of holographic tools and techniques, including the use of fiber optic components for remote optical access;[5] however, only a small fraction of the work performed in the area of holo-interferometry deals with making measurements within cavities. Moreover, most attempts to record holograms over extended areas in confined spaces have met with limited success, mainly because of the problems associated with panoramic imaging. Some of these problems have been addressed during the development of radial metrology and panoramic holography.

2. RADIAL METROLOGY

Radial metrology combines standard optical techniques with a panoramic annular lens (PAL) for cavity measurement. Originally patented by Dr. Pal Greguss of the Technical University of Budapest and currently available through Optechnology Inc., Huntsville, Alabama, the PAL consists of a single piece of glass with spherical surfaces that produces a flat annular image of the entire 360 degree surround of the optical axis of the lens. As illustrated in

0-8194-0705-4/92/$4.00

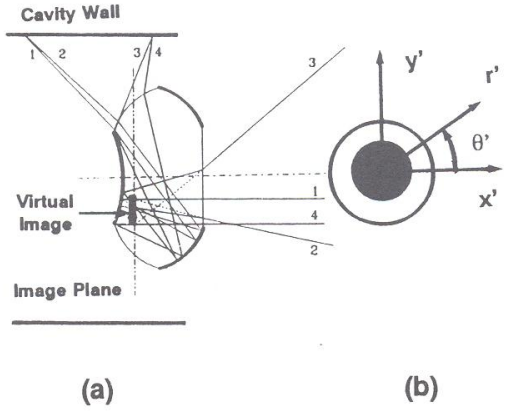

Figure 1. (a) Ray diagram for a PAL; (b) Coordinate systems (x',y') and (r',θ') have been superimposed on the annular image to help define the image plane.

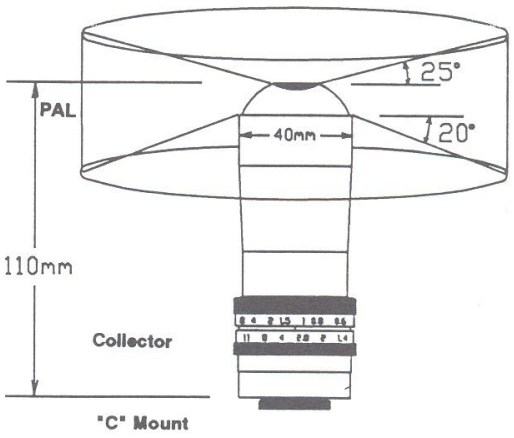

Figure 2. The dimensions and field of view for a 38 mm-diameter PAL imaging system. Figure provided courtesy of Optechnology, Inc., Huntsville, AL.

Figure 1, light is reflected and refracted within the lens to form a virtual image. This image must be transferred to an image capturing device using a collector lens. This is illustrated in Figure 2 which shows the schematic of a commercially available PAL imaging system. The system includes a 38 mm-diameter PAL mounted with an f/1.4, 25 mm focal length collector lens. The field of view extends from about -20 degrees below the lens to about 25 degrees above the lens; a "C" mount is included so that the system can be attached to a standard video camera. The PAL can also be used with a compound lens system or, by itself, to illuminate the wall of a cavity. The most outstanding attributes of the PAL are that there are no moving parts, the area surrounding the lens can be viewed simultaneously, and the depth of focus extends from its surface to infinity. These attributes make it possible to holographically record and measure displacements within cavities using the technique of panoramic holo-interferometry.

3. PANORAMIC HOLOGRAPHY AND HOLO-INTERFEROMETRY

Prior research has demonstrated that a single PAL can be used to construct a panoramic holocamera.[6] The device relies on a high resolution film wrapped around the PAL and may be used to record double-exposure and time-average holograms. The holocamera has an advantage that holograms can be reconstructed in white light; however, it is limited in its real-time capabilities, since the film must be removed and developed after each holographic recording. An alternate approach was recently suggested in which real-time holo-interferometric fringe patterns are recorded within a cavity using two opposing collinear panoramic annular lenses.[7] Some interesting interferometric fringe patterns were produced in both of these studies but discussions of these patterns were limited to qualitative evaluations.

This paper expands on the prior research performed in the area of panoramic holo-interferometry by developing the parameters and equations required to quantitatively analyze holo-interferometric fringes. The research is being conducted for NASA's Marshall Space Flight Center and is expected to provide a new inspection capability for the Space Shuttle Main Engine program. Panoramic holo-interferometry may be used to verify the condition of space hardware after manufacturing, to perform inservice inspections following ground test engine firings, and to predict potential failure sites during refurbishment between shuttle flights.

The ability to measure submicron deformations caused by small perturbations in temperature, pressure and mechanical loads within cavities will be of tremendous importance to the program in general. Double-exposure and real-time techniques could be used to detect surface and subsurface cracks, voids, debonds and material anomalies. Time-average methods may help to identify resonant frequencies and to determine exact vibration amplitudes in a vibrating engine; panoramic holography could also be applied for flow visualization, plasma diagnostics, pattern recognition, process control, and particle sizing.

4. ANALYSIS

The PAL produces an annular image; the cartesian (x',y') and polar (r',θ') coordinate systems used to analyze this image are shown superimposed on Figure 1b. Figure 3, on the other hand, defines the cartesian (x,y,z) and cylindrical (r,θ,z) coordinate systems used to describe object space.

Referring to Figure 3, it is assumed that two opposing collinear PALs are aligned with their optical axes along the z-direction. Coherent light is projected by one PAL from the source point S to a point P located on the wall of a cavity. The image of P is observed by the second PAL at point O. For analysis purposes, unit vectors $\hat{e}_1$ and $\hat{e}_2$ are shown in the direction of illumination and in the direction of observation, respectively.

These vectors are important in analyzing the holographic fringes produced when two reconstructed hologram images corresponding to an undeformed and deformed surface are superimposed. In this case,

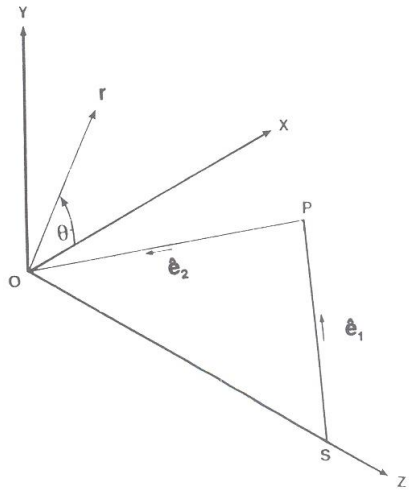

Figure 3. Cartesian (x,y,z) and cylindrical (r,θ,z) coordinate systems used to describe object space.

$$n\lambda = \mathbf{g} \cdot \mathbf{d} \qquad (1)$$

where n is the fringe order number, λ is the wavelength of the coherent light used to record and reconstruct the hologram and **d** is the displacement vector of the surface point under consideration. The sensitivity vector **g** is defined by $(\hat{e}_2 - \hat{e}_1)$.

The observed displacement fringes are due to the change in optical path length which occurs between recordings. These path length changes give rise to a distribution of phase differences between the reconstructed wavefronts which results in areas of constructive or destructive interference and is seen as a set of light and dark fringes. As discussed above, the component of displacement measured at each point depends upon the location of the source and on the point of observation; the displacement vector is projected along the sensitivity vector which coincides with the angle bisector of $\hat{e}_1$ and $\hat{e}_2$.

A better physical understanding of the situation at hand may be gained by expressing Equation (1) in terms of cartesian coordinates. With the displacement vector given by

$$\mathbf{d} = u\,\hat{i} + v\,\hat{j} + w\,\hat{k} \qquad (2)$$

and subscripts s, o and p used to denote the source, observation and surface coordinates, respectively, the phase-displacement relation given by Equation (1) becomes

$$\boldsymbol{g} \cdot \boldsymbol{d} = \left[\frac{(x_s-x)}{R_s}+\frac{(x_o-x)}{R_o}\right] u + \left[\frac{(y_s-y)}{R_s}+\frac{(y_o-x)}{R_o}\right] v + \left[\frac{(z_s-z)}{R_s}+\frac{(z_o-z)}{R_o}\right] w = n\lambda \qquad (3)$$

where

$$R_s = [(x_s-x)^2+(y_s-y)^2+(z_s-z)^2]^{1/2} \qquad R_o = [(x_o-x)^2+(y_o-y)^2+(z_o-z)^2]^{1/2}$$

In general, the displacement vector is projected along a different direction for each model point and it becomes necessary to take several holograms to obtain the necessary information to fully establish the three cartesian components (u,v,w) for every model point. One strategy is to change the source and/or observation point to obtain at least three independent equations in the three unknown displacement components. In practice, it is easier to change the observation direction. Equations are generated when the reconstructed image is viewed from different observation positions located on one or more holograms. A substantial amount of numerical analysis is necessary to analyze this general situation. Data reduction can be minimized, however, by making modifications in the recording and reconstruction phases.

For example, if a relatively flat surface is intentionally oriented normal to the angle bisector of $\hat{e}_1$ and $\hat{e}_2$, the interferometer senses only the out-of-plane displacement component, w, and Equation (3) becomes,

$$n\lambda = 2w\ (\cos\ \varphi) \qquad (4)$$

where 2ϕ is the angle between the propagation vectors in the directions of illumination and observation.

Holographic interferograms can also be optically superimposed to isolate the in-plane displacement components using the holographic-moire method.[8,9] In this method, the object is illuminated by two beams oriented symmetrically with respect to the surface normal, say at an angle δ. Two holo-interferometric fringe patterns, usually referred to as component patterns, result from the dual beam illumination. The fringe orders can be numerically subtracted or the component patterns can be optically superimposed to produce a moire. The superposition is characterized by the equation,

$$n\lambda = 2u\ (\sin\delta) \qquad (5)$$

where n is the difference between the fringe order numbers in the component patterns, λ is the wavelength used to record and reconstruct the holo-interferograms, and u is the displacement component measured in the plane formed by the propagation vectors from the two sources and oriented perpendicular to their angle bisector.

In summary, Equations (1) and (3) can be used to measure displacement projected along a sensitivity vector and optics can be positioned to obtain selected displacement components. However, the situation is slightly more complex when holo-interferograms are recorded using a PAL system. In this case, fringe loci must be established in the image plane. Displacements may only be computed by taking into account the geometry and the optical properties of each PAL.

The illumination and observation directions for a PAL may be described with respect to a circular ring defined by the loci of the points of intersection of rays corresponding to the upper and lower field angles. The lens shown in Figure 2, for example, has an upper field angle of 25 degrees and a lower field angle of -20 degrees. The ring is called the offset and is defined relative to the front of the lens; the axial offset is the distance measured from the circle to the front of the lens while the radial offset is measured perpendicular to the optical axis and equals the radius of the circle. The axial offset, a_o, is defined as positive when the offset lies behind the front surface of the PAL; whereas, the radial offset, r_o, is positive when each point forming the circle lies on the opposite side of the

optical axis from the surface being viewed or illuminated. For the lens shown in Figure 2, a_o = 0.4 cm (0.157") and r_o = 0.05 cm (0.019"). The offset defines the source points when the PAL is used to illuminate a cavity; it defines the observation points when the cavity is imaged by a PAL.

5. EXPERIMENTAL

Experiments were performed with the setup shown in Figure 4 to illustrate that holo-interferometric fringe patterns can be recorded with the PAL system for cases in which the cavity moves relative to the recording system. Two 38 mm (1.5") diameter PALs, with optical characteristics analogous to those contained in the imaging system shown in Figure 2, were spaced at a distance of 3.175 mm (0.125") apart and positioned with their optical axes aligned with the z-axis of the coordinate system shown in Figure 3. The origin of the coordinate systems was located in the offset plane of the PAL subsequently used for imaging. A circular brass pipe with an inner radius, R, equal to 69.85 mm (2.75") and a wall thickness of 3.0 mm (0.117"), was mounted on a kinematic stage and positioned around the PALs with its longitudinal axis also along z. The inner surface of the pipe was painted white, and coherent light (λ = 514 nm) was projected onto the inner wall of a 50.8 mm (2.0") long section of the pipe using a collimated beam passed through one of the PALs. An image of the pipe in its initial position was captured using a second PAL. A collector lens was used to convey the virtual image, formed within the PAL itself, to a CCD camera and computer system. As shown in the figure, a hologram of the wavefronts emerging from the second PAL was recorded using a thermoplastic holocamera positioned behind the collector lens.*

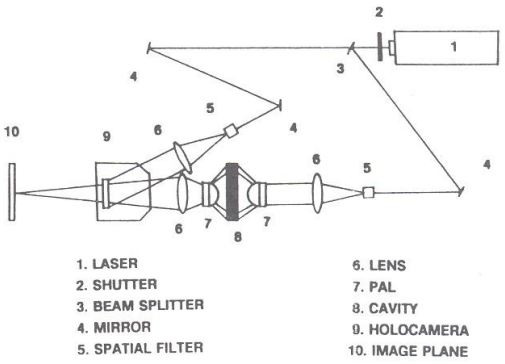

Figure 4. Experimental setup for recording real-time holograms. A CCD camera is used to acquire images.

Figure 5 shows a reconstruction of the fringe pattern recorded in real time after the pipe was translated along the x-axis, through a displacement u equal to 0.0053 mm (0.0002"). When the pipe is translated along the y-axis, through a displacement v equal to 0.0053 mm (0.0002"), the pattern shown in Figure 5 results with fringe field rotated by 90 degrees. Figure 6 was obtained by holographically recording the pipe in its initial position and then translating it along the z-axis, through a displacement w equal to 0.0038 mm (0.00015").

These results may be qualitatively evaluated. For the pipe and the PAL system described, the sensitivity vector lies primarily along the radial direction; it is perpendicular to the surface towards the center of the annular image, becoming progressively more inclined with respect to the normal as the limiting field angles are approached. These characteristics are evident in Figures 5 and 6. In Figure 5, zero order fringes are observed at θ equal to 90 and 270 degrees where the sensitivity vector is perpendicular to the imposed displacement. Maximum fringe order numbers occur at θ equal to 0 and 180 degrees, at points where the directions of the sensitivity vector and displacement vector coincide. The deviation in the direction of the sensitivity vector from that of the surface normal is evident from the fringe gradient observed at these angular locations. This deviation accounts for the fringe pattern shown in Figure 6, in which a zero order fringe appears toward the center of the annulus; fringe orders increase monotonically from the inner to the outer boundary.

* The holocamera can also be positioned between the collector lens and the PAL, or in the image plane. However, the latter condition causes excessive noise during reconstruction, since anomalies such as dirt and pits in the thermoplastic are recorded along with the image of the cavity.

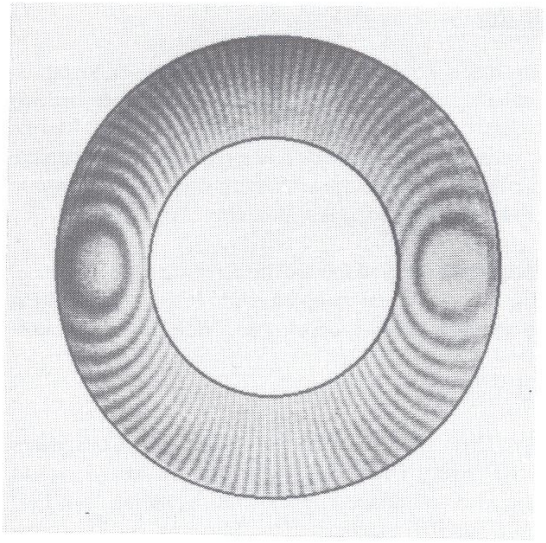

Figure 5. Holo-interferometric fringe pattern for a pipe section translated along x.

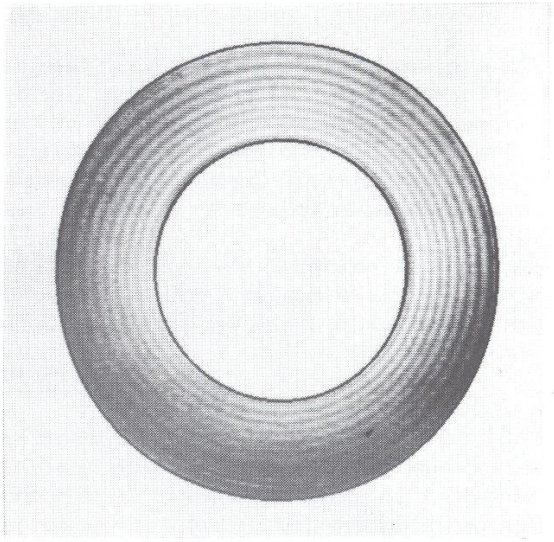

Figure 6. Holo-interferometric fringe pattern for a pipe section translated along z.

Quantitative evaluation is slightly more difficult, but can be accomplished using linearization algorithms developed to improve human viewing during visual inspections with PAL systems. Linearization is accomplished by 'rolling' the annular image along its outer circumference and moving all the pixels between the contact point and the center of the image to an appropriate location on a vertical line in the final rectangular image.[10] Figures 7 and 8 show the results of applying the linearization algorithms to the second and first quadrants of the images contained in Figures 5 and 6, respectively. The resulting fringe patterns are compared to those predicted analytically by Equations (1) and (3).

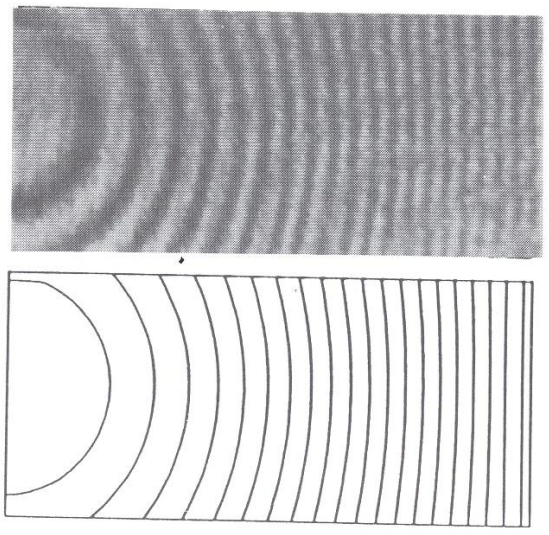

Figure 7. The second quadrant of the image shown in Figure 5 is linearized and compared with theory.

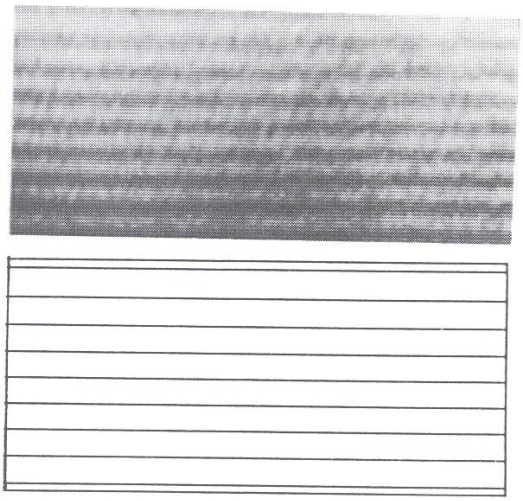

Figure 8. The first quadrant of the image shown in Figure 6 is linearized and compared with theory.

6. CONCLUSIONS

This paper has described a method in which measurements are made within a cavity using real-time holographic recording and a panoramic viewing system. The method, called panoramic holo-interferometry, relies on two collinear panoramic annular lenses to record holographic fringes caused by rigid body displacements. Results indicate that the panoramic system records displacements along sensitivity vectors which lie predominately along the radial direction. Tangential displacements can not be measured; however, since the sensitivity vectors have varying components along the optical axis, the system is sensitive to displacement along that direction.

Future work will be driven by new developments in PAL technology and directed toward the construction of practical systems designed to measure a particular displacement component. When coupled with image linearization techniques, these systems will allow qualitative evaluation and quantitative analysis of panoramic holo-interferograms.

7. ACKNOWLEDGEMENTS

PAL research has been funded by NASA's Marshall Space Flight Center and the Alabama Space Grant Consortium under Contract Nos. NAG8-686, NAG-159, and NAS8-36955 Delivery Order 124. The authors would like to acknowledge the interest and support of several personnel at the Marshall Space Flight Center including Jack Lee, Director; Bill Lucas, former Director; Ann Whitaker, Ken Woodis, and Ron Beshears of the Materials and Processes Laboratory; John McCarty, Eric Hyde, Gary Lyles, and Jay Nichols of the Propulsion Laboratory; James Moses of the Research and Technology Office; and, Jonathan Campbell of the Space Sciences Laboratory who first entertained our proposal to "Change The World's Perspective."

8. REFERENCES

1. Erf, R.K., Holographic Nondestructive Testing, Academic Press, N.Y., (1974).
2. Vest, C.M., Holographic Interferometry, Wiley Publishers, N.Y., (1979).
3. Abramson, N., The Making and Evaluation of Holograms, Academic Press, N.Y., (1981).
4. Ranson, W.F., Sutton, M.A., Peters, W.H., "Holographic and laser speckle interferometry," Chapter 8 in Handbook on Experimental Mechanics, Edited by A.S. Kobayashi, Society for Experimental Mechanics, Inc., Prentice-Hall, N.J., 1987.
5. Gilbert, J.A., Dudderar, T.D., "The uses of fiber optics to enhance and extend the capabilities of holographic interferometry," Proc. of SPIE's Institute on Holography as Science and Technology, Tatabanya, Hungary, June 2-5, 1990.
6. Greguss, P., "Panoramic holocamera for tube and borehole inspection," Proc. of the Int. Seminar on Laser and Optoelectronic Technology in Industry - A State of the Art Review, Xiamen, P.R.C., June 25-27, 1986.
7. Gilbert, J.A., Greguss, P., Kransteuber, A.S., "Holo-interferometric patterns recorded through a panoramic annular lens," Proc. of SPIE's International UNESCO Seminar on 3-D Holography, Volume 1238, entitled 3-D Holography '89, Kiev, USSR, September 5-8, 1989.
8. 13. Hung, Y.Y., Taylor, C.E., "Measurement of surface displacements normal to the line of sight by holo-moire interferometry," J. Appl. Mech., 42, (1975), pp. 1-4.
9. Sciammarella, C.A., Gilbert, J.A., A holographic-moire technique to obtain separate patterns for components of displacement, Exp. Mech., 16, (1976), pp. 215-220.
10. Matthys, D.R., Gilbert, J.A., Puliparambil, J., "Endoscopic inspection using a panoramic annular lens," Proc. of SPIE's 1991 International Symposium on Optical & Optoelectronic Applied Science & Engineering, San Diego, California, July 21-26, 1991.